RESEARCH ARTICLE

Rapid detection and structural characterization of verapamil metabolites in rats by UPLC–MSE and UNIFI platform

Chunyan Zhu[1] | Mimi Wan[2] | Huilin Cheng[1] | Hui Wang[2] | Mingshe Zhu[1,3] | Caisheng Wu[1] (ID)

[1] Fujian Provincial Key Laboratory of Innovative Drug Target Research and State Key Laboratory of Cellular Stress Biology, School of Pharmaceutical Sciences, Xiamen University, Xiamen, China

[2] China Solution Center, Waters Technologies (Shanghai) Corporation, Shanghai, China

[3] MassDefect Technologies, Princeton, New Jersey, USA

Correspondence
Hui Wang, Waters Technologies (Shanghai) Corporation, 13 Building, No. 1000, Jinhai Road, Pudong New Area, Shanghai City, China.
Email: hui_wang@waters.com

Caisheng Wu, School of Pharmaceutical Sciences Xiamen University, Xiang'an South Road, Xiang'an District, Xiamen City, China.
Email: wucsh@xmu.edu.cn

Abstract

High-resolution mass spectrometry (HRMS) is an important technology for studying biotransformations of drugs in biological systems. In order to process complex HRMS data, bioinformatics, including data-mining techniques for identifying drug metabolites from liquid chromatography/high-resolution mass spectrometry (LC/HRMS) or multistage mass spectrometry (MS^n) datasets as well as elucidating the detected metabolites' structure by spectral interpretation software, are important tools. Data-mining technologies have widely been used in drug metabolite identification, including mass defect filters, product ion filters, neutral-loss filters, control sample comparisons and extracted ion chromatographic analysis. However, the metabolites identified by current different technologies are not the same, indicating the importance of technique integration for efficient and complete identification of metabolic products. In this study, a universal, high-throughput workflow for identifying and verifying metabolites by applying the drug metabolite identification software UNIFI is reported, to study the biotransformation of verapamil in rats. A total of 71 verapamil metabolites were found in rat plasma, urine and faeces, including two metabolites that have not been reported in the literature. Phase I metabolites of verapamil were identified as *N*-demethylation, *O*-demethylation, *N*-dealkylation and oxidation and dehydrogenation metabolites; phase II metabolites were mainly glucuronidation and sulfate conjugates, indicating that UNIFI software could be effective and valuable in identifying drug metabolites.

KEYWORDS

UNIFI, UPLC–MSE, verapamil metabolites

1 | INTRODUCTION

Drug metabolism research spans the entire drug development process. Rapid, accurate and complete identification of drug metabolites in biological systems can improve the understanding of drugs or candidate compounds' biotransformation pathways, which might also facilitate the determination of metabolic 'soft sites'. This information is valuable for optimizing the structure of lead compounds, selecting drugs with high metabolic stability and exploring the drugs' possible pharmacological or toxicological mechanisms. High-performance liquid chromatography–high-resolution mass spectrometry (HPLC–HRMS) (Song, Jin, Du, Cao, & Xu, 2016) has high resolution, accuracy and sensitivity, is fast scanning and involves multistage mass spectrometry (MS^n). It is a powerful tool for analysing drug metabolites and can be used to obtain HRMS and MS^n data from potential metabolic products in biological samples using a simple, universal collection method. However, the mass spectrometry data collected by the device contains a large amount of data relating to endogenous compounds. Therefore,

approaches to efficiently and comprehensively identify the information of interest as well as to analyse metabolic products in post-processing, have become one of the key issues in HPLC–HRMS applications. (Gao, Wu, & Feng, 2019; Martano, Mugoni, Dal Bello, Santoro, & Medana, 2015; Scheidweiler, Jarvis, & Huestis, 2015; Song et al., 2016)

In recent years, there have been numerous studies of post-processing techniques for high-resolution mass spectrometry, and the reported techniques can be divided into three main types. The first is detection based on known or predictable metabolic pathways, such as the conventional metabolic products formed by hydroxylation and *N*-dealkylation. Since the molecular weights of these products can be predicted, high-resolution extracted ion chromatography (HR–EIC) can be used for targeted analysis of expected metabolite ions (Xing, Zang, Zhang, & Zhu, 2015), thereby making detection relatively simple. The second is post-processing techniques based on HRMS data, including mass defect filters (MDF) (Geng et al., 2016; Ruan & Zhu, 2010; Shang et al., 2017; Tian et al., 2015; Zhang, Zhang, Ray, & Zhu, 2009; Zhang, Zhu, Ray, Ma, & Zhang, 2008; Zhu et al., 2006), isotope pattern filters and background subtraction (BS) (Chen et al., 2016; Wu et al., 2016; Zeng, Duan, Chen, Li, & Liu, 2017; Zhang, Gan, Shu, & Humphreys, 2015). The third is post-processing techniques based on MS^n data, including product ion filters (Cuyckens, Hurkmans, Castro-Perez, Leclercq, & Mortishire-Smith, 2009; Ma, Wen, Ruan, & Zhu, 2008; Ruan et al., 2008; Zhang & Yang, 2008), neutral-loss filters (NLF) (Liu et al., 2014; Ruan et al., 2008; Yao et al., 2017) and mass spectral tree similarity filter technique (Jin, Wu, Zhang, & Li, 2013; Vaniya & Fiehn, 2015; Wang, Wu, Qin, & Zhang, 2014). All of these techniques address the issue of identification or verification of metabolic products. However, current reports show that the metabolites identified by different apporaches are not the same, indicating the importance of technology integration for efficient and complete identification of metabolic products.

In this report, we describe a strategy for a universal, high-throughput workflow for identifying and verifying metabolic products. In detail, ultra-performance liquid chromatography–tandem mass spectrometry (UPLC–MS^E) was used to collect mass spectrometry information about verapamil compounds' metabolites, while the UNIFI software platform was used for data processing. This combination of UPLC–MSE data acquisition technology and the integrated data-processing functions of the UNIFI platform was proved to rapidly detect small metabolites from dealkylation, to allow direct binary comparison for easy metabolite identification and even to enable the exploration of unknown metabolites, which might be suitable for high-throughput screening and analysis of reactive metabolites or metabolic soft-spots in future drug discovery.

2 | MATERIALS AND METHODS

2.1 | Chemicals and reagents

Verapamil (98%, MB1346) was purchased from the National Institute for the Control of Pharmaceutical and Biological Products (NICPBP),

methanol and acetonitrile of LC/MS grade were purchased from Fisher Scientific (Waltham, MA, USA) and analytical grade formic acid (99%) was obtained from Sigma-Aldrich (USA). Purified water used in the study was produced by a Milli-Q integral water purification system (Millipore Direct-Q UV, Bedford, MA, USA).

2.2 | Animals

Three male Wistar rats, weighing 220 ± 20 g, were obtained from the Shanghai Laboratory Animal Company (Shang Hai, China). All rats were housed under standard conditions (12 h dark–light cycle; temperature $25 \pm 2°C$; humidity 50–75%) with access to food and water. They were fasted for 12 h with free access to water before the experiment.

2.3 | Drug administration and biological sample preparation

Verapamil was dissolved in saline solution. The rats were given an oral dose of 30 mg/kg body weight. After the oral administration of verapamil, blood samples (0.5 ml) were taken from the suborbital venous plexus of rats at 0.25, 0.75, 1.5, 3, 6, 10 and 12 h. Each sample was centrifuged at 4000 rpm for 10 min to obtain plasma samples. Urine and faeces samples were collected 0–10 and 10–24 h after oral administration. Control plasma, urine and faeces samples were collected before administration. All samples were stored at −80°C before analysis.

The plasma samples (0.5 mL) were placed in 5 mL centrifuge tubes, and 2 mL methanol was added to precipitate protein. The urine samples (1 mL) were transferred to 10 mL capped centrifuge tubes and 4 mL methanol was added. After mixing for 30 s, the sample tubes were centrifuged at 4500 rpm for 10 min, and then the supernatants of all plasma samples and 1 mL of supernatant from each urine sample were transferred into a new 10 mL polypropylene centrifuge tube and evaporated to dryness using nitrogen at 37°C. Finally, the plasma and urine residues were re-dissolved with 100 and 200 μL acetonitrile–water (30:70, v/v) respectively, and ultrasonicated for 2 min, before being centrifuged at 12,000 rpm for 10 min. The plasma supernatant was directly injected into the LC–MS system, and the urine supernatant was diluted 1:10 before analysis.

The faeces samples (0.2 g) were transferred to 10 mL centrifuge tubes and mixed with 400 μL of water, followed by the addition of 800 μL of methanol solution, ultrasonicated for 15 min and subsequently centrifuged at 12,000 rpm for 10 min to obtain the supernatant. The supernatant was removed and dried. The residue was reconstituted in methanol (50 μL) and diluted 1:10 and then injected into the system for analysis.

2.4 | Instruments and conditions

The chromatographic equipment consisted of a UPLC system (Waters Acquity UPLC I-Class). Separations were carried out on an Acquity

UPL HSS T3 Column (2.1 × 100 mm, 1.8 μm) maintained at 35°C. A 0.1% FA aqueous solution (solvent A) and 0.1% FA acetonitrile (solvent B) were used as the mobile phases. The flow rate was set at 0.3 mL/min with a linear gradient as follows: 0–0.2 min, 5–5% B; 0.2–3 min, 5–15% B; 3–8 min, 15–24% B; 8–16 min, 24–38% B; 16–20 min, 38–95% B; 20–22 min, 95% B; 22–24 min, 95–5% B. The injection volumes of rat plasma, urine and faeces were 0.5, 0.1 and 0.2 μL, respectively.

Mass spectrometry was performed on a Waters Xevo G2-XS QTOF, equipped with an electrospray ionization source in both positive and negative ion modes. Acquisition mode was MS^E; capillary voltage, 3.0 kV; source offset, 80; sampling cone, 40.0; desolvation temperature, 500°C; source temperature, 150°C; desolvation gas flow, 850 L/h; cone gas flow, 50 L/h; and acquisition time, 24 min. Data was acquired using MS^E, and the mass was corrected using an external reference (Lock-Spray).

2.5 | Data processing

Data were processed using UNIFI (1.8.2) software. The UNIFI core is an information library that allows researchers to map and navigate their metabolite identification data using novel visualizations, as well as in tabular or combined views. The data-processing workflow is shown in Figure 1. First, the Binary Compare function was applied to identify potential metabolites that were not present or were present at low ion intensities in the corresponding control samples. The relative intensity threshold was set at 3 or 5, and metabolites meeting this requirement could be screened out. EIC was then used to find common, predictable metabolites. The characteristic fragment ions of verapamil metabolites were m/z 303.2072, 260.1657 and 165.0917. Therefore, compounds with m/z 303.2072, 260.1657 or 165.0917 were probably verapamil metabolites. MDF, product ion filters and NLF were applied to detect unpredictable metabolites. MDF incorporating an intelligent dealkylation function is capable of rapidly detecting small metabolites from dealkylation, with no false negative results. The NLF function was applied to search for two-phase metabolites.

For instance, we could search for possible glucuronic acid conjugates by setting a parameter at 176.0321 in the UNIFI software. In UNIFI, neutral loss can be set in the method or identified after processing. Finally, the detected metabolites' structures were determined or characterized using MassFragment, which is part of UNIFI's spectral interpretation function. This is the main function used to automatically perform secondary fragmentation analysis of parent drugs and metabolites. Using this function, researchers can quickly verify whether the fragmentation path is reasonable.

3 | RESULTS AND DISCUSSION

3.1 | UPLC–MSE analysis of metabolites

In this study, verapamil's metabolic profile was studied using UPLC–MS^E with the UNIFI platform, while the number of detected compounds was compared with BS, MDF and MDF + dealkylation (shown in Figure 2). After being processed by BS, MDF and MDF + dealkylation and UNIFI, the numbers of verapamil metabolites screened in rat plasma were 9529, 225, 934 and 341 compounds (shown in Supporting Table S1–S12) respectively from the total database (14,283 compounds), while most of them were false positive compounds. Only 37 true compounds were obtained after BS treatment, accounting for 0.39% of the total. Some 6.67% (21 compounds) and 2.25% (37 compounds) positive compounds after processing by MDF and MDF+ dealkylation were screened, respectively. In short, 93% of screened compounds were false positive compounds. As screening efficiency was poor, a large number of manual operations were required. However, the UNIFI platform automatically screened 341 compounds from the verapamil plasma database (14,283 compounds), of which 37 (accounting for 10.85%) were true verapamil metabolites. Compared with the other three methods, UNIFI technology showed great screening effect. Furthermore, the verapamil metabolites in urine and faeces were also processed using BS, MDF, MDF + dealkylation and UNIFI. The experimental results revealed that 32 (accounting for 6.43%), 12 (accounting for 27.91%), 19 (accounting
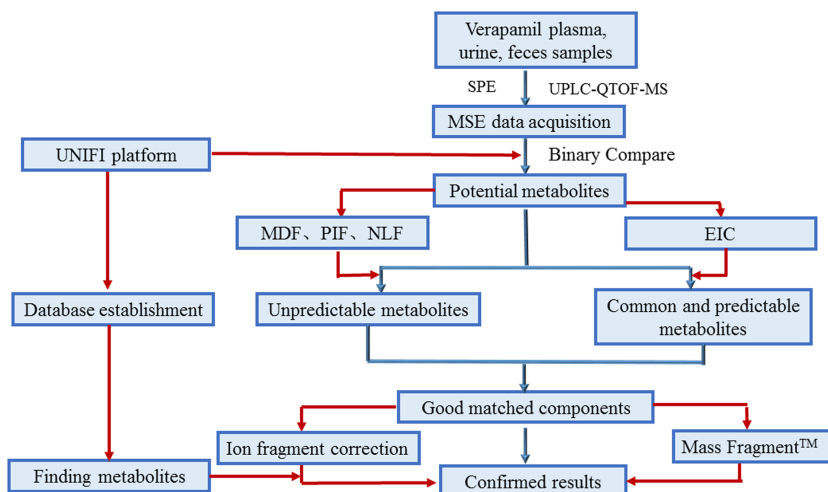

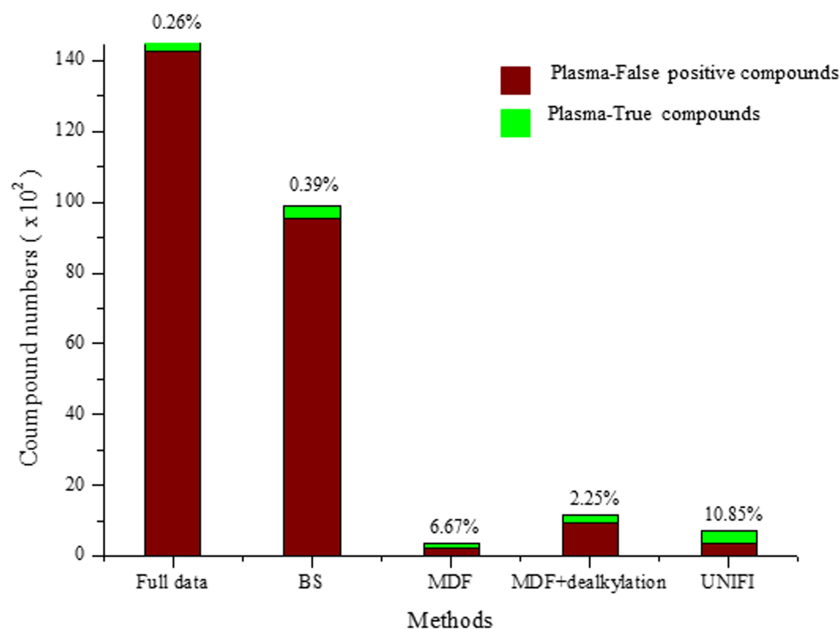**FIGURE 1** Shows the workflow of extracts identification process

FIGURE 2 Comparison of the number of compounds detected in the plasma using each data processing method. The solid fills (wine and green) indicate the total number of compounds detected, and the green fills indicate the number of true compounds detected, accounting for 0.26, 0.39, 6.67, 2.25 and 10.85% of the total, respectively

for 6.03%) and 32 (accounting for 20.13%) true compounds (total screened compounds 498, 43, 315 and 159) were obtained, respectively, in urine. By calculation, the effective rates of compounds screened from faeces were 7.69, 14.43, 6.05 and 17.49% using each data processing method (total screened compounds 598,194, 727 and 263), respectively. It reveals that UNIFI could effectively reduce the false positive rate, with false rates of only 89.15, 79.87 and 82.51% in plasma, urine and faeces, in comparison with the other three methods with most of screened false rates above 92% (shown in Supporting Figure S1).

The metabolites identified by UNIFI are summarized in Table 1, showing the data from parent compounds and drug metabolites. A total of 71 verapamil metabolites were found in rat plasma, urine and faeces. The major metabolic pathways in rats are N- and O-demethylation and N-dealkylation. Two of the detected metabolites had not been reported in the literature. In detail, 37, 31 and 45 metabolites were found in plasma, urine and faeces, respectively, but only nine metabolites (M4-1, M4-2, M4-3, M5-3, M5-6, M7, M11-3, M11-5 and M12-5) were detected simultaneously in three substrates. According to the reported literature, *in vivo* verapamil metabolism could be affected by a number of enzymes. For example, CYP3A4, CYP3A4 and CYP1A2 were reported to be the main enzymes responsible for verapamil N-dealkylation and CYP2C isoenzymes (particularly CYP2C9) were mainly involved in verapamil O-demethylation (Busse, Cosme, Kroemer, & Eichelbaum, 1995; Sun, Zhang, & Zhong, 2004). The enzymes responsible for the three main initial pathways of verapamil metabolism were identified. N-Dealkylated metabolites were the main metabolites in plasma and urine, while N- and O-demethylated compounds were the main metabolites in faeces (Reder-Hilz et al., 2004). Verapamil and its N-dealkylated metabolites might be further metabolized by O-demethylation (Sun et al., 2004). In short, significant differences in the types and amounts of metabolites detected from the three matrices may be due to differences in the metabolic main enzymes affecting verapamil metabolism in different matrices.

3.2 | Identification of metabolite M12-5

Most of the metabolites had similar structures. The verapamil structure and fragment ions are shown in Figure 3. Verapamil had the theoretical $[M + H]^+$ ion at m/z 455.2910 ($C_{27}H_{38}N_2O_4$, error 0 mDa) in positive ion mode, which eluted at 15.01 min. Its fragment ions were also obtained at m/z 303.2072, 260.1657, 165.0917 and 150.0672. Therefore, it could be inferred that the ions at m/z 303.2072, 260.1657, 165.0917 and 150.0672 were characteristic product ions of verapamil (M0). In order to identify metabolites, these ions were used for structural elucidation of metabolites with similar skeletons. For example, M12-5 belonged to a verapamil metabolite and had a retention time of 14.66 min. A base peak ion at m/z 441.2748 ($C_{26}H_{36}N_2O_4$, error − 0.4 mDa) was observed. There were also fragment ions at m/z 289.1912, 260.1648, 165.0909 and 150.0672. Fragment ions at m/z 260.1648, 165.0909 and 150.0672 were similar to the product ions of the parent compound. The fragment ion at m/z 289.1912 was the result of m/z 303.2065 loss CH_2 (14.0153 Da), which suggested that the A and B rings of verapamil had not undergone O-demethylation. These observations provided unambiguous evidence that M12-5 was verapamil with loss of CH_2, owing to the N-demethylation of verapamil, and it agreed with MS fragment information.

3.3 | Separation and analysis of isomers

In the present study, the UNIFI platform applied to data from ultra-performance liquid chromatography coupled with quadrupole time-of-flight mass spectrometry (UPLC–MS^E–QTOF) was used to isolate and identify the verapamil metabolite isomers. Fifteen group isomers were discovered, including metabolites M1, M2, M4, M5, M6, M8, M9, M10, M11, M12, M14, M17, M18, M19 and M22. To illustrate the specific operating principle, four representative isomer samples were listed. Four chromatographic peaks could be detected with the molecular

TABLE 1 Summary of verapamil metabolites in plasma, urine and faeces

Name	Metabolic pathway	Formula	[M + H]+	Retention time (min)	Mass error (mDa)	Reaponse Plasma 0.25 h	1.5 h	12 h	Urine 0–12 h	Feces 0–12 h	12–24 h
M0	Parent	$C_{27}H_{38}N_2O_4$	455.290	15.01	0.00	+++	+++	++	+++	+	n.d.
M1-1	N-Dealkylation + N-demethylation + O-demethylation (B ring) + glucuronide conjugation	$C_{21}H_{30}N_2O_8$	439.208	5.10	0.00	+	++	++	++	n.d.	n.d.
M1-2	N-Dealkylation + 2 × demethylation + glucuronide conjugation	$C_{21}H_{30}N_2O_8$	439.207	5.20	−0.40	+	++	++	++	n.d.	n.d.
M1-3	N-dealkylation + N-demethylation + O-demethylation (B ring) + glucuronide conjugation	$C_{21}H_{30}N_2O_8$	439.207	5.72	−0.50	n.d.	+	+	+	n.d.	n.d.
M1-4	N-Dealkylation + 2 × demethylation + glucuronide conjugation	$C_{21}H_{30}N_2O_8$	439.208	5.97	0.10	n.d.	+	n.d.	++	n.d.	n.d.
M2-1	N-Dealkylation + O-demethylation (B ring) + glucuronide conjugation	$C_{22}H_{32}N_2O_8$	453.223	5.32	−0.30	+++	+++	+++	+++	n.d.	n.d.
M2-2	N-Dealkylation + O-demethylation (B ring) + glucuronide conjugation	$C_{22}H_{32}N_2O_8$	453.223	5.41	−0.10	++	+++	++	+++	+++	n.d.
M2-3	N-Dealkylation + O-demethylation (B ring) + glucuronide conjugation	$C_{22}H_{32}N_2O_8$	453.223	5.91	−0.50	+	++	+	++	n.d.	n.d.
M2-4	N-Dealkylation + O-demethylation (B ring) + glucuronide conjugation	$C_{22}H_{32}N_2O_8$	453.223	6.17	−0.30	+	++	+	++	n.d.	n.d.
M3	Verapamil-$C_{17}H_{24}N_2O_2$ (cleavage)−CH_2−H_2	$C_9H_{10}O_2$	151.075	7.46	0.00	+++	+++	+	+++	n.d.	n.d.
M4–1	N-Dealkylation + O-demethylation(B ring)	$C_{16}H_{24}N_2O_2$	277.190	8.05	−0.60	+	+	+	+++	+++	n.d.
M4–2	N-Dealkylation + O-demethylation(B ring)	$C_{16}H_{24}N_2O_2$	277.191	8.40	−0.60	+	+	+	++	+++	n.d.
M4–3	N-Dealkylation + N-demethylation	$C_{16}H_{24}N_2O_2$	277.191	9.74	−0.10	++	+++	++	+++	+	n.d.
M5–1	oxidation and demethylation to $C_{17}H_{26}N_2O_2$ area	$C_{26}H_{36}N_2O_5$	457.270	9.07	0.20	n.d.	n.d.	n.d.	1792	917	n.d.
M5–2	Oxidation + demethylation	$C_{26}H_{36}N_2O_5$	457.270	9.29	−0.10	+	+	+	n.d.	n.d.	n.d.
M5–3	Oxidation and demethylation to $C_{17}H_{26}N_2O_2$ area	$C_{26}H_{36}N_2O_5$	457.270	10.20	0.00	+	n.d.	n.d.	+	+	n.d.
M5–4	Oxidation + demethylation	$C_{26}H_{36}N_2O_5$	457.270	11.50	−0.10	+	+	n.d.	n.d.	+	n.d.
M5–5	Oxidation and demethylation to $C_{17}H_{26}N_2O_2$ area	$C_{26}H_{36}N_2O_5$	457.269	12.34	−0.40	++	++	++	n.d.	n.d.	n.d.
M5–6	Oxidation to A ring or carbon next to it + N-demethylation	$C_{26}H_{36}N_2O_5$	457.269	13.53	−0.30	++	++	+	+	++	n.d.
M6-1	2 × Demethylation to $C_{17}H_{26}N_2O_2$ area + glucuronide conjugation	$C_{31}H_{42}N_2O_{10}$	603.291	9.58	0.00	++	++	++	++	n.d.	n.d.
M6-2	2 × Demethylation + glucuronide conjugation	$C_{31}H_{42}N_2O_{10}$	603.292	10.06	0.20	n.d.	+	n.d.	n.d.	n.d.	n.d.
M6-3	2 × Demethylation + glucuronide conjugation	$C_{31}H_{42}N_2O_{10}$	603.293	10.34	1.30	n.d.	+	+	n.d.	n.d.	n.d.
M6-4	O-demethylation (A ring) + N-Demethylation + glucuronide conjugation	$C_{31}H_{42}N_2O_{10}$	603.291	10.73	−0.20	+++	+++	+++	++	n.d.	n.d.
M6-5	O-Demethylation (A ring) + demethylation to $C_{17}H_{26}N_2O_2$ + glucuronide conjugation	$C_{31}H_{42}N_2O_{10}$	603.291	11.33	0.00	+	+	+	+	n.d.	n.d.
M7	N-Dealkylation	$C_{17}H_{26}N_2O_2$	291.207	10.03	−0.10	+++	+++	+	+++	++	n.d.

(Continues)

TABLE 1 (Continued)

Name	Metabolic pathway	Formula	[M + H]$^+$	Retention time (min)	Mass error (mDa)	Plasma 0.25 h	1.5 h	12 h	Urine 0–12 h	Feces 0–12 h	12–24 h
M8-1	Oxidation to $C_{17}H_{26}N_2O_2$ area	$C_{27}H_{38}N_2O_5$	471.285	10.44	−0.20	+	+	n.d.	+	n.d.	n.d.
M8-2	Oxidation	$C_{27}H_{38}N_2O_5$	471.285	12.54	−0.10	n.d.	n.d.	n.d.	n.d.	++	n.d.
M8-3	Oxidation to $C_{17}H_{26}N_2O_2$ area	$C_{27}H_{38}N_2O_5$	471.285	12.76	0.00	++	++	++	n.d.	n.d.	n.d.
M8-4	Oxidation to A ring or carbon next to it	$C_{27}H_{38}N_2O_5$	471.285	13.80	−0.40	++	++	+	n.d.	n.d.	n.d.
M8-5	Oxidation	$C_{27}H_{38}N_2O_5$	471.285	13.92	−0.20	++	++	+	+	n.d.	n.d.
M8-6	Oxidation	$C_{27}H_{38}N_2O_5$	471.286	15.39	0.30	+	+	+	n.d.	n.d.	n.d.
M9-1	Demethylation + glucuronide conjugation	$C_{32}H_{44}N_2O_{10}$	617.308	9.74	0.60	+	+	+	+	n.d.	n.d.
M9-2	O-Demethylation (A ring) + glucuronide conjugation	$C_{32}H_{44}N_2O_{10}$	617.307	10.58	−0.20	++	++	++	+	n.d.	n.d.
M9-3	Demethylation + glucuronide conjugation	$C_{32}H_{44}N_2O_{10}$	617.307	11.48	0.40	+	+	n.d.	n.d.	n.d.	n.d.
M10-1	O-Demethylation (B ring) + 2 × demethylation (A ring)	$C_{24}H_{32}N_2O_4$	413.243	10.39	−0.40	n.d.	n.d.	n.d.	n.d.	154193	n.d.
M10-2	2 × Demethylation (A ring) + O-demethylation (B ring)	$C_{24}H_{32}N_2O_4$	413.243	10.67	−0.40	n.d.	n.d.	n.d.	n.d.	++	n.d.
M10-3	O-Demethylation (A ring) + 2 × demethylation to $C_{17}H_{26}N_2O_2$ area	$C_{24}H_{32}N_2O_4$	413.243	11.35	−0.50	n.d.	n.d.	n.d.	n.d.	++	n.d.
M10-4	O-Demethylation (A ring) + 2 × demethylation to $C_{17}H_{26}N_2O_2$ area	$C_{24}H_{32}N_2O_4$	413.243	11.66	−0.30	n.d.	n.d.	n.d.	n.d.	+	n.d.
M10-5	2 × Demethylation (A ring) + N-demethylation	$C_{24}H_{32}N_2O_4$	413.243	12.09	0.00	n.d.	n.d.	n.d.	n.d.	+++	n.d.
M11-1	O-Demethylation (A ring) + demethylation to $C_{17}H_{26}N_2O_2$ area	$C_{25}H_{34}N_2O_4$	427.259	11.57	−0.60	n.d.	n.d.	n.d.	n.d.	+	n.d.
M11-2	2 × Demethylation (A ring)	$C_{25}H_{34}N_2O_4$	427.259	12.25	0.00	n.d.	n.d.	n.d.	n.d.	+++	n.d.
M11-3	2 × Demethylation to $C_{17}H_{26}N_2O_2$ area	$C_{25}H_{34}N_2O_4$	427.258	12.80	−0.80	+	+	+	+	++	n.d.
M11-4	2 × Demethylation to $C_{17}H_{26}N_2O_2$ area	$C_{25}H_{34}N_2O_4$	427.259	13.11	−0.20	+	+	+	n.d.	n.d.	n.d.
M11-5	O-Demethylation (A ring) + N-demethylation	$C_{25}H_{34}N_2O_4$	427.259	13.24	−0.20	+	+	+	++	+++	n.d.
M11-6	O-Demethylation (A ring) + demethylation to $C_{17}H_{26}N_2O_2$ area	$C_{25}H_{34}N_2O_4$	427.259	13.62	−0.10	n.d.	n.d.	n.d.	n.d.	+	n.d.
M12-1	O-Demethylation (B ring)	$C_{26}H_{36}N_2O_4$	441.274	13.11	−0.40	n.d.	n.d.	n.d.	+	++	n.d.
M12-2	O-demethylation (B ring)	$C_{26}H_{36}N_2O_4$	441.274	13.42	−0.30	++	++	++	n.d.	n.d.	n.d.
M12-3	O-demethylation (A ring)	$C_{26}H_{36}N_2O_4$	441.275	13.44	−0.30	n.d.	n.d.	n.d.	+	+++	n.d.
M12-4	O-demethylation (A ring)	$C_{26}H_{36}N_2O_4$	441.275	13.90	−0.30	n.d.	n.d.	n.d.	n.d.	++	n.d.
M12-5	N-Demethylation	$C_{26}H_{36}N_2O_4$	441.274	14.66	−0.40	+++	+++	+++	+++	++	n.d.
M13	verapamil-$C_{11}H_{15}NO_2$(cleavage) + O + 2 × (−H_2)	$C_{16}H_{19}NO_3$	274.144	16.50	−0.20	+++	++	++	n.d.	+	n.d.
M14-1	N-Dealkylation + 2 × demethylation (B ring)	$C_{15}H_{22}N_2O_2$	263.175	6.31	−0.30	n.d.	n.d.	n.d.	n.d.	++	n.d.
		$C_{15}H_{22}N_2O_2$	263.175	7.76	−0.20	n.d.	n.d.	n.d.	+	++	n.d.

(Continues)

TABLE 1 (Continued)

Name	Metabolic pathway	Formula	[M + H]$^+$	Retention time (min)	Mass error (mDa)	Reaponse Plasma 0.25 h	1.5 h	12 h	Urine 0–12 h	Feces 0–12 h	12–24 h
M14-2	N-Dealkylation + N-demethylation + O-demethylation (B ring)										
M14-3	N-Dealkylation + 2 × demethylation	$C_{15}H_{22}N_2O_2$	263.175	8.13	−0.40	n.d.	n.d.	n.d.	+	++	n.d.
M15	Oxidation to A ring or carbon next to it + N-demethylation + O-demethylation (B ring)	$C_{25}H_{34}N_2O_5$	443.255	11.71	1.00	n.d.	n.d.	n.d.	+	++	n.d.
M16	5 × Demethylation	$C_{22}H_{28}N_2O_4$	385.212	8.44	−0.10	n.d.	n.d.	n.d.	n.d.	+	n.d.
M17-1	2 × Demethylation (A ring) + 2 × demethylation to $C_{17}H_{26}N_2O_2$ area	$C_{23}H_{30}N_2O_4$	399.228	8.60	0.40	n.d.	n.d.	n.d.	n.d.	+	n.d.
M17-2	O-Demethylation (B ring) + N-demethylation + 2 × demethylation (A ring)	$C_{23}H_{30}N_2O_4$	399.228	10.21	−0.30	n.d.	n.d.	n.d.	n.d.	+++	n.d.
M17-3	O-Demethylation (B ring) + N-demethylation + 2 × demethylation (A ring)	$C_{23}H_{30}N_2O_4$	399.227	10.51	−0.40	n.d.	n.d.	n.d.	n.d.	++	n.d.
M18-1	3 × Demethylation-dehydrogenation	$C_{24}H_{30}N_2O_4$	411.227	9.41	−0.40	n.d.	n.d.	n.d.	n.d.	+	n.d.
M18-2	3 × Demethylation-dehydrogenation	$C_{24}H_{30}N_2O_4$	411.227	9.55	−0.50	n.d.	n.d.	n.d.	n.d.	+	n.d.
M18-3	O-demethylation (B ring) + N-demethylation + O-demethylation (A ring) + dehydrogenation	$C_{24}H_{30}N_2O_4$	411.228	10.06	−0.10	n.d.	n.d.	n.d.	n.d.	+++	n.d.
M18-4	O-Demethylation (B ring) + N-demethylation + O-demethylation (A ring) + dehydrogenation	$C_{24}H_{30}N_2O_4$	411.228	10.79	−0.30	n.d.	n.d.	n.d.	n.d.	++	n.d.
M18-5	3 × Demethylation-dehydrogenation	$C_{24}H_{30}N_2O_4$	411.227	11.10	−0.60	n.d.	n.d.	n.d.	n.d.	+	n.d.
M19-1	2 × Demethylation to $C_{11}H_{17}NO_2$ area + dehydrogenation	$C_{25}H_{32}N_2O_4$	425.243	11.20	−0.30	n.d.	n.d.	n.d.	n.d.	++	n.d.
M19-2	2 × Demethylation to $C_{11}H_{17}NO_2$ area + dehydrogenation	$C_{25}H_{32}N_2O_4$	425.243	11.42	−0.20	n.d.	n.d.	n.d.	n.d.	++	n.d.
M19-3	O-Demethylation (A ring) + N-demethylation + dehydrogenation	$C_{25}H_{32}N_2O_4$	425.244	11.99	0.10	n.d.	n.d.	n.d.	n.d.	+++	n.d.
M19-4	O-Demethylation (A ring) + N-demethylation + dehydrogenation	$C_{25}H_{32}N_2O_4$	425.243	12.76	−0.20	n.d.	n.d.	n.d.	n.d.	+++	n.d.
M20	3 × Oxidation	$C_{27}H_{38}N_2O_7$	503.275	11.52	−0.20	n.d.	n.d.	n.d.	n.d.	+	n.d.
M21	Oxidation + demethylation (to A ring or C next to it) + sulfation	$C_{26}H_{36}N_2O_8S$	537.226	12.95	−0.10	n.d.	n.d.	n.d.	n.d.	+	n.d.
M22-1	Demethylation + dehydrogenation	$C_{26}H_{34}N_2O_4$	439.259	12.34	0.00	n.d.	n.d.	n.d.	n.d.	++	n.d.
M22-2	Demethylation + dehydrogenation	$C_{26}H_{34}N_2O_4$	439.259	12.50	0.20	n.d.	n.d.	n.d.	n.d.	+	n.d.

Note: n.d., not detected; +, peak area < 10^3; ++, peak area 10^5; +++, peak area 10^6.

composition $C_{22}H_{32}N_2O_8$ (M2-1, M2-2, M2-3 and M2-4, shown in Figure 4), which eluted at 5.32, 5.41, 5.91 and 6.17 min, respectively, with the same [M + H]$^+$ ions at m/z 453.2228 (C22H32N2O8, error − 0.3 mDa). The fragment ions at m/z 277.1910, 246.1487, 234.1362 and 246.1487 were derived from the O-demethylation (B ring) of m/z 260.1645 by loss of CH_2 (14.0158 Da); m/z 234.1362 was 43.0548 Da less than m/z 277.1910, which was derived from N-dealkylation. In addition, the fragment ion m/z 453.2331 was

176.0421 Da (higher than m/z 277.1910), suggesting that it was a glucuronide conjunction. Metabolite M2-1 was, therefore, assumed to have undergone N-dealkylation, O-demethylation (B ring) and glucuronide conjugation of the verapamil prototype, which agreed with MS fragment information. Further analysis indicated that the four metabolites were isomers, because they exhibited the same protonated ion at m/z 277.1910 and had characteristic neutral losses of 176.0421 Da. Their different retention times on the UPLC system
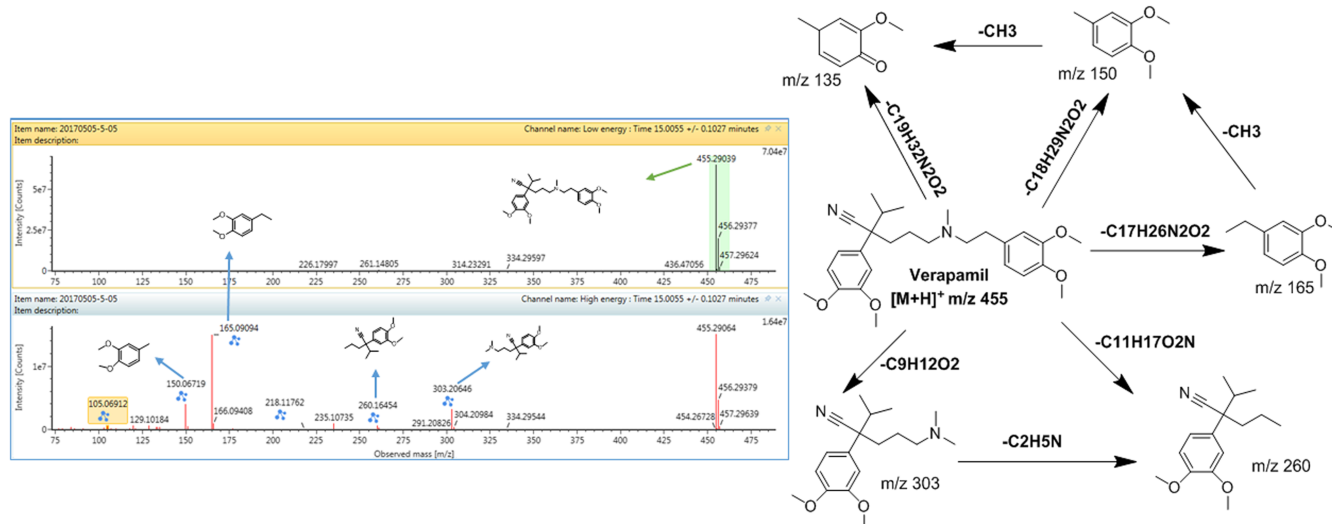
FIGURE 3 MS2 fragmentation pattern of verapamil. Arrows in the molecular structure of the drug demonstrate the resulting cationic species upon collision induced dissociation and detailed fragmentation pathway of verapamil based on Xevo G2-XS QTOF MS2 and MS3 experiments
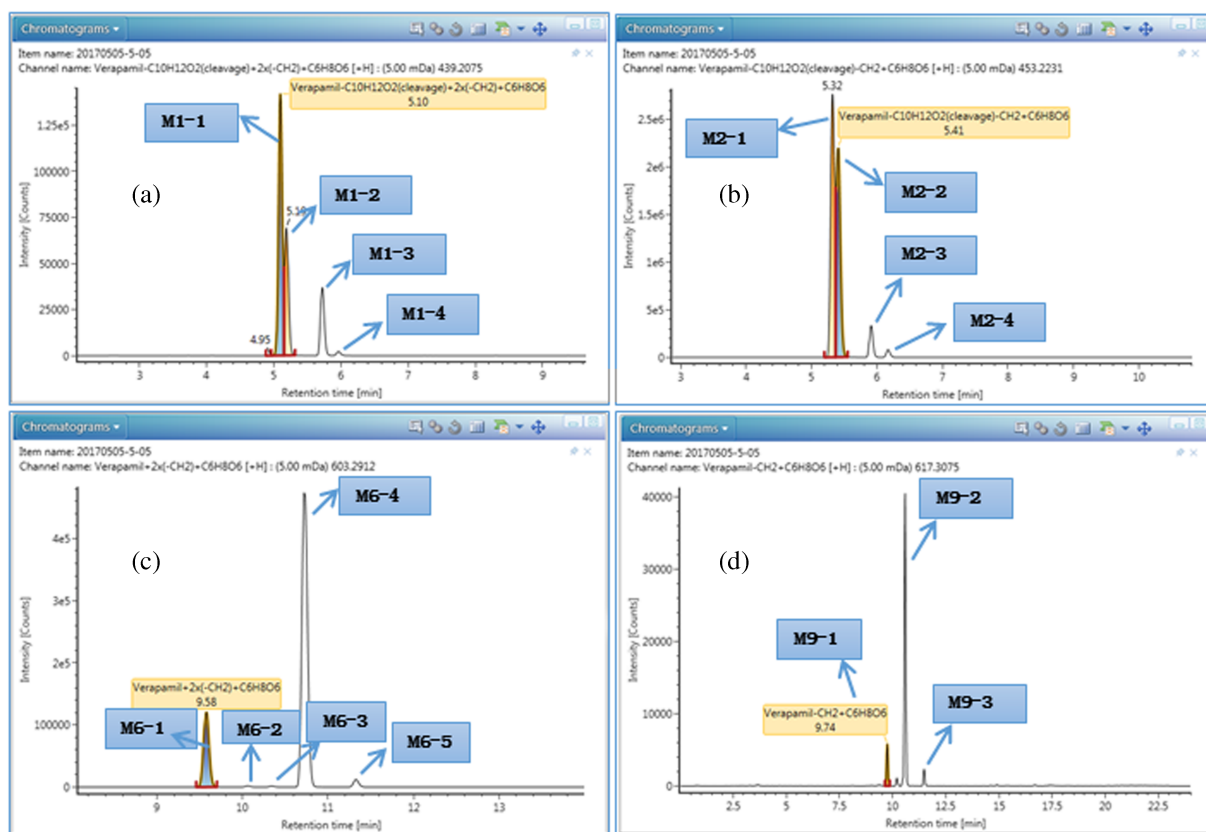

FIGURE 4 Based on UPLC separation technology and UNIFI software data processing, the separation and identification of multiple pairs of verapamil metabolites isomers were obtained. (a), (b), (c), (d) are the four pairs isomers of verapamil glucuronic acid conjugates

indicated that isomerization took place in the conjugation reaction in different positions.

3.4 | Metabolites M3 and M13

Metabolites M3 and M13 had not previously been reported in the literature, and their structures were elucidated. Metabolite M3 eluted at

7.46 min and had its $[M + H]^+$ ion at m/z 151.0753 ($C_9H_{10}O_2$, error 0 mDa). M3 could be detected in plasma and urine. Metabolite M13 was eluted at 16.50 min, with $[M + H]^+$ at m/z 274.1435 ($C_{16}H_{19}NO_3$, error −0.2 mDa). In the ESI–MS2 spectra of M13, product ions at m/z 247.1435, m/z 231.0881 and m/z 189.0782 were observed (shown in Supporting Figure S2), providing evidence for demethylation and oxidation occurred on N.
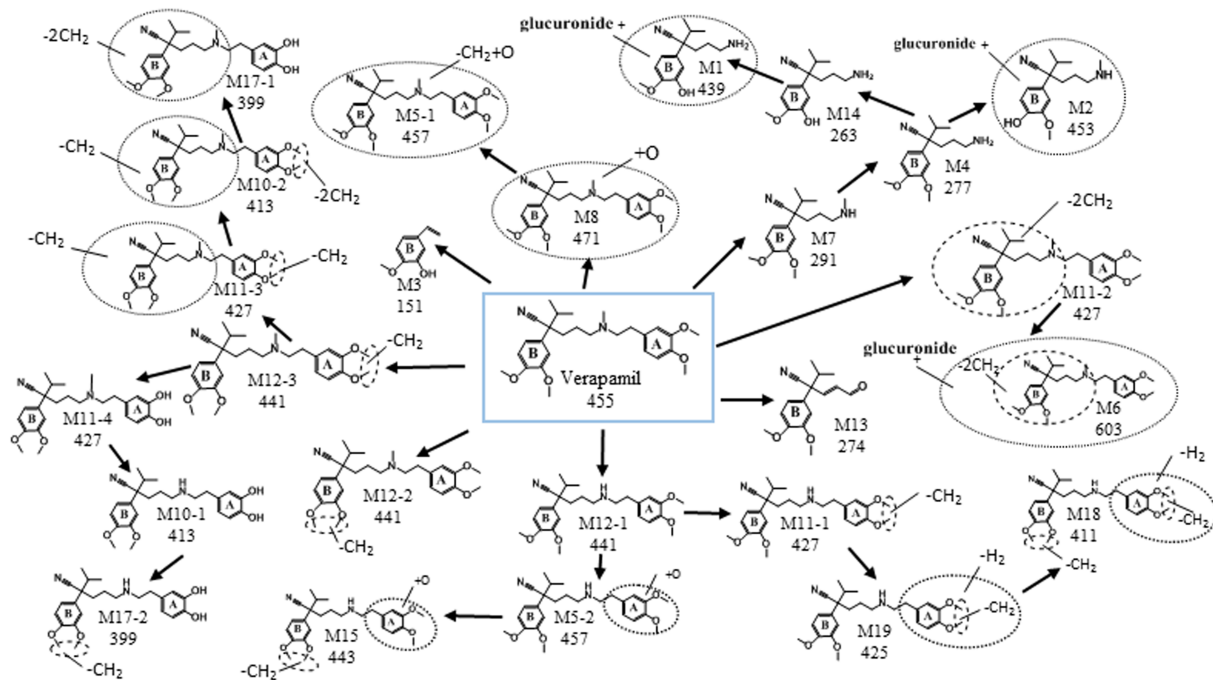
FIGURE 5   The possible metabolic pathway of verapamil

3.5 | Summary of the metabolic pathway of verapamil

In this study, 71 metabolites (including the prototype compound) with different structures were observed and identified in rats following oral administration of verapamil. The proposed metabolic pathway of verapamil in rats is presented in Figure 5. Both phase I and II reactions were involved in verapamil metabolism. For instance, 37 verapamil metabolites were detected in rat plasma samples, including 21 phase I metabolites and 16 phase II metabolites. Thirty-one metabolites of verapamil were found in rat urine. Of these, 18 metabolites were phase I metabolites, and 13 were phase II metabolites. In rat faeces, 45 verapamil metabolites were detected; 44 were phase I metabolites and one was a phase II metabolite. The phase I metabolic pathway consisted of N-demethylation, N-dealkylation, oxidation, dehydrogenation and hydroxylation. Products from this primary metabolism further underwent glucuronidation and sulfation in phase. Verapamil metabolism appears to include the following major pathways: verapamil was first biotransformed into M3, M7 (dealkylation product), M8 (oxidation product), M11 (di-demethylation product), M12 (demethylation product), M13 and so on. Subsequently, a series of bioreactions occurred, including demethylation (M4, M10), oxidation (M5), glucuronide conjugation (M6, M9) and sulfation (M21), as well as their complicated biotransformation products. For instance, M17 was identified as arising from the demethylation of M10-5. M15 was identified as a demethylation product of M5-6. M11 was converted into M19 by dehydrogenation and then was biotransformed into M18. M4 was further converted into M14 by demethylation, and then conjugation glucuronide reactions occurred on M14 to produce its conjugation product M1. Other metabolites were generated by verapamil,

undergoing multiple reactions. It is notable that the phase II metabolites in rat faeces consist only of a sulfation product, M21.

4 | CONCLUSIONS

UNIFI integrates a number of data-mining tools for drug metabolite detection and can perform automated spectral interpretation for the structural determination of metabolites using an HRMS-based approach. Among the verapamil metabolites identified, 54 metabolites were phase I and 17 were phase II, such as glucuronide and sulfate conjugates. Some of the metabolites detected have not been reported in the literature and are currently undergoing structural analysis. The major metabolic pathways in rats are N- and O-demethylation and N-dealkylation. Products from this primary metabolism undergo further glucuronidation and sulfation. In addition, multiple minor metabolites from hydroxylation were detected.

The combination of UPLC–MS[E] data acquisition technology and the integrated data-processing functions of the UNIFI platform provides several advances when finding and identifying metabolites. First, MDF incorporated with the intelligent dealkylation function is capable of rapidly detecting small metabolites from dealkylation, with no false negative results. Second, the Binary Compare function allows comparison of ions between experimental and control samples so that metabolites can be easily identified. Third, the MassFragment™ function enables automated interpretation of the mass spectra of unknown metabolites. Finally, the workflow of generic data acquisition, combined with data-mining and data interpretation functions, is well suited for high-throughput screening and analysis of reactive metabolites and metabolic soft-spots in a drug discovery setting.

CONFLICT OF INTEREST

The authors declare no conflicts of interest.

ORCID

Caisheng Wu https://orcid.org/0000-0002-8554-1564

REFERENCES

Busse, D., Cosme, J., Kroemer, P. B. H. K., & Eichelbaum, M. (1995). Cytochromes of the P450 2C subfamily are the major enzymes involved in the *O*-demethylation of verapamil in humans. *Naunyn-Schmiedeberg's Archives of Pharmacology*, *353*, 116–121.

Chen, C., Wohlfarth, A., Xu, H., Su, D., Wang, X., Jiang, H., & Zhu, M. (2016). Untargeted screening of unknown xenobiotics and potential toxins in plasma of poisoned patients using high-resolution mass spectrometry: Generation of xenobiotic fingerprint using background subtraction. *Analytica Chimica Acta*, *944*, 37–43. https://doi.org/10.1016/j.aca.2016.09.034

Cuyckens, F., Hurkmans, R., Castro-Perez, J. M., Leclercq, L., & Mortishire-Smith, R. J. (2009). Extracting metabolite ions out of a matrix background by combined mass defect, neutral loss and isotope filtration. *Rapid Communications in Mass Spectrometry*, *23*, 327–332. https://doi.org/10.1002/rcm.3881

Gao, Y., Wu, S., & Feng, L. (2019). Rapid and direct determination of fatty acids and glycerides profiles in *Schisandra chinensis* oil by using UPLC–Q/TOF-MS(E). *Journal of Chromatography B*, *1104*, 157–167.

Geng, P., Sun, J., Zhang, M., Li, X., Harnly, J. M., & Chen, P. (2016). Comprehensive characterization of C-glycosyl flavones in wheat (*Triticum aestivum* L.) germ using UPLC–PDA-ESI/HRMS(n) and mass defect filtering. *Journal of Mass Spectrometry*, *51*, 914–930. https://doi.org/10.1002/jms.3803

Jin, Y., Wu, C. S., Zhang, J. L., & Li, Y. F. (2013). A new strategy for the discovery of epimedium metabolites using high-performance liquid chromatography with high resolution mass spectrometry. *Analytica Chimica Acta*, *768*, 111–117. https://doi.org/10.1016/j.aca.2013.01.012

Liu, M., Zhao, S., Wang, Z., Wang, Y., Liu, T., Li, S., & Tu, P. (2014). Identification of metabolites of deoxyschizandrin in rats by UPLC–Q-TOF–MS/MS based on multiple mass defect filter data acquisition and multiple data processing techniques. *Journal of Chromatography B*, *949–950*, 115–126.

Ma, L., Wen, B., Ruan, Q., & Zhu, M. (2008). Rapid screening of glutathione-trapped reactive metabolites by linear ion trap mass spectrometry with isotope pattern-dependent scanning and postacquisition data mining. *Chemical Research in Toxicology*, *21*, 1477–1483. https://doi.org/10.1021/tx8001115

Martano, C., Mugoni, V., Dal Bello, F., Santoro, M. M., & Medana, C. (2015). Rapid high performance liquid chromatography–high resolution mass spectrometry methodology for multiple prenol lipids analysis in zebrafish embryos. *Journal of Chromatography a*, *1412*, 59–66. https://doi.org/10.1016/j.chroma.2015.07.115

Reder-Hilz, B., Ullrich, M., Ringel, M., Hewitt, N., Utesch, D., Oesch, F., & Hengstler, J. G. (2004). Metabolism of propafenone and verapamil by cryopreserved human, rat, mouse and dog hepatocytes: Comparison with metabolism *in vivo*. *Naunyn Schmiedebergs Archives of Pharmacology*, *369*, 408–417. https://doi.org/10.1007/s00210-004-0875-z

Ruan, Q., & Zhu, M. S. (2010). Investigation of bioactivation of ticlopidine using linear ion trap/orbitrap mass spectrometry and an improved mass defect filtering technique. *Chemical Research in Toxicology*, *23*, 909–917. https://doi.org/10.1021/tx1000046

Ruan, Q., Peterman, S., Szewc, M. A., Ma, L., Cui, D., Humphreys, W. G., & Zhu, M. (2008). An integrated method for metabolite detection and identification using a linear ion trap/Orbitrap mass spectrometer and multiple data processing techniques: Application to indinavir metabolite detection. *Journal of Mass Spectrometry*, *43*, 251–261. https://doi.org/10.1002/jms.1311

Scheidweiler, K. B., Jarvis, M. J., & Huestis, M. A. (2015). Nontargeted SWATH acquisition for identifying 47 synthetic cannabinoid metabolites in human urine by liquid chromatography–high-resolution tandem mass spectrometry. *Analytical and Bioanalytical Chemistry*, *407*, 883–897. https://doi.org/10.1007/s00216-014-8118-8

Shang, Z., Xin, Q., Zhao, W., Wang, Z., Li, Q., Zhang, J., & Cong, W. (2017). Rapid profiling and identification of puerarin metabolites in rat urine and plasma after oral administration by UHPLC–LTQ-Orbitrap mass spectrometer. *Journal of Chromatography B*, *1068–1069*, 180–192.

Song, G., Jin, M., Du, Y., Cao, L., & Xu, H. (2016). UPLC–QTOF–MS/MS based screening and identification of the metabolites in rat bile after oral administration of imperatorin. *Journal of Chromatography B*, *1022*, 21–29.

Sun, L., Zhang, S.-q., & Zhong, D.-f. (2004). *In vitro* identification of metabolites of verapamil in rats liver microsomes. *Acta Pharmacologica Sinica*, 121–128.

Tian, T., Jin, Y., Ma, Y., Xie, W., Xu, H., Zhang, K., & Du, Y. (2015). Identification of metabolites of oridonin in rats with a single run on UPLC–triple-TOF–MS/MS system based on multiple mass defect filter data acquisition and multiple data processing techniques. *Journal of Chromatography B*, *1006*, 80–92.

Vaniya, A., & Fiehn, O. (2015). Using fragmentation trees and mass spectral trees for identifying unknown compounds in metabolomics. *TrAC Trends in Analytical Chemistry*, *69*, 52–61.

Wang, C.-H., Wu, C.-S., Qin, H.-L., & Zhang, J.-L. (2014). Rapid discovery and identification of 68 compounds in the active fraction from Xiao–Xu–Ming decoction (XXMD) by HPLC–HRMS and MTSF technique. *Chinese Chemical Letters*, *25*, 1648–1652.

Wu, C., Zhang, H., Wang, C., Qin, H., Zhu, M., & Zhang, J. (2016). An integrated approach for studying exposure, metabolism, and disposition of multiple component herbal medicines using high-resolution mass spectrometry and multiple data processing tools. *Drug Metabolism and Disposition*, *44*, 800–808. https://doi.org/10.1124/dmd.115.068189

Xing, J., Zang, M., Zhang, H., & Zhu, M. (2015). The application of high-resolution mass spectrometry-based data-mining tools in tandem to metabolite profiling of a triple drug combination in humans. *Analytica Chimica Acta*, *897*, 34–44. https://doi.org/10.1016/j.aca.2015.09.034

Yao, C. L., Yang, W. Z., Si, W., Shen, Y., Zhang, N. X., Chen, H. L., & Guo, D. A. (2017). An enhanced targeted identification strategy for the selective identification of flavonoid *O*-glycosides from *Carthamus tinctorius* by integrating offline two-dimensional liquid chromatography/linear ion-trap-Orbitrap mass spectrometry, high-resolution diagnostic product ions/neutral loss filtering and liquid chromatography-solid phase extraction-nuclear magnetic resonance. *Journal of Chromatography a*, *1491*, 87–97. https://doi.org/10.1016/j.chroma.2017.02.041

Zeng, S. L., Duan, L., Chen, B. Z., Li, P., & Liu, E. H. (2017). Chemicalome and metabolome profiling of polymethoxylated flavonoids in Citri Reticulatae Pericarpium based on an integrated strategy combining background subtraction and modified mass defect filter in a Microsoft Excel Platform. *Journal of Chromatography A, 1508*, 106–120. https://doi.org/10.1016/j.chroma.2017.06.015

Zhang, H., & Yang, Y. (2008). An algorithm for thorough background subtraction from high-resolution LC/MS data: Application for detection of glutathione-trapped reactive metabolites. *Journal of Mass Spectrometry, 43*, 1181–1190. https://doi.org/10.1002/jms.1390

Zhang, H., Zhu, M., Ray, K. L., Ma, L., & Zhang, D. (2008). Mass defect profiles of biological matrices and the general applicability of mass defect filtering for metabolite detection. *Rapid Communications in Mass Spectrometry, 22*, 2082–2088. https://doi.org/10.1002/rcm.3585

Zhang, H., Zhang, D., Ray, K., & Zhu, M. (2009). Mass defect filter technique and its applications to drug metabolite identification by high-resolution mass spectrometry. *Journal of Mass Spectrometry, 44*, 999–1016. https://doi.org/10.1002/jms.1610

Zhang, H., Gan, J., Shu, Y. Z., & Humphreys, W. G. (2015). High-resolution mass spectrometry-based background subtraction for identifying protein modifications in a complex biological system: detection of acetaminophen-bound microsomal proteins including argininosuccinate synthetase. *Chemical Research in Toxicology, 28*, 775–781. https://doi.org/10.1021/tx500526s

Zhu, M., Ma, L., Zhang, D., Ray, K., Zhao, W., Humphreys, W. G., & Zhang, H. (2006). Detection and characterization of metabolites in biological matrices using mass defect filtering of liquid chromatography/high resolution mass spectrometry data. *Drug Metabolism and Disposition, 34*, 1722–1733. https://doi.org/10.1124/dmd.106.009241

SUPPORTING INFORMATION

Additional supporting information may be found online in the Supporting Information section at the end of the article.